Supplementary Information

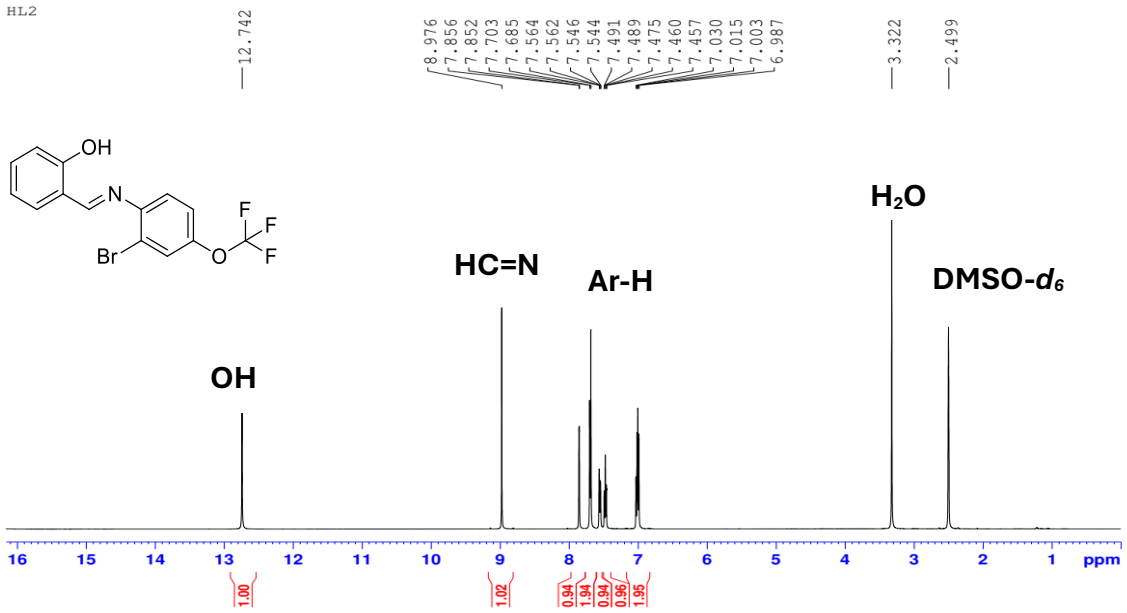

Figure S1: ^{1}H NMR spectrum of the **HL** recorded at 298 K using (500 MHz, DMSO-d_6)

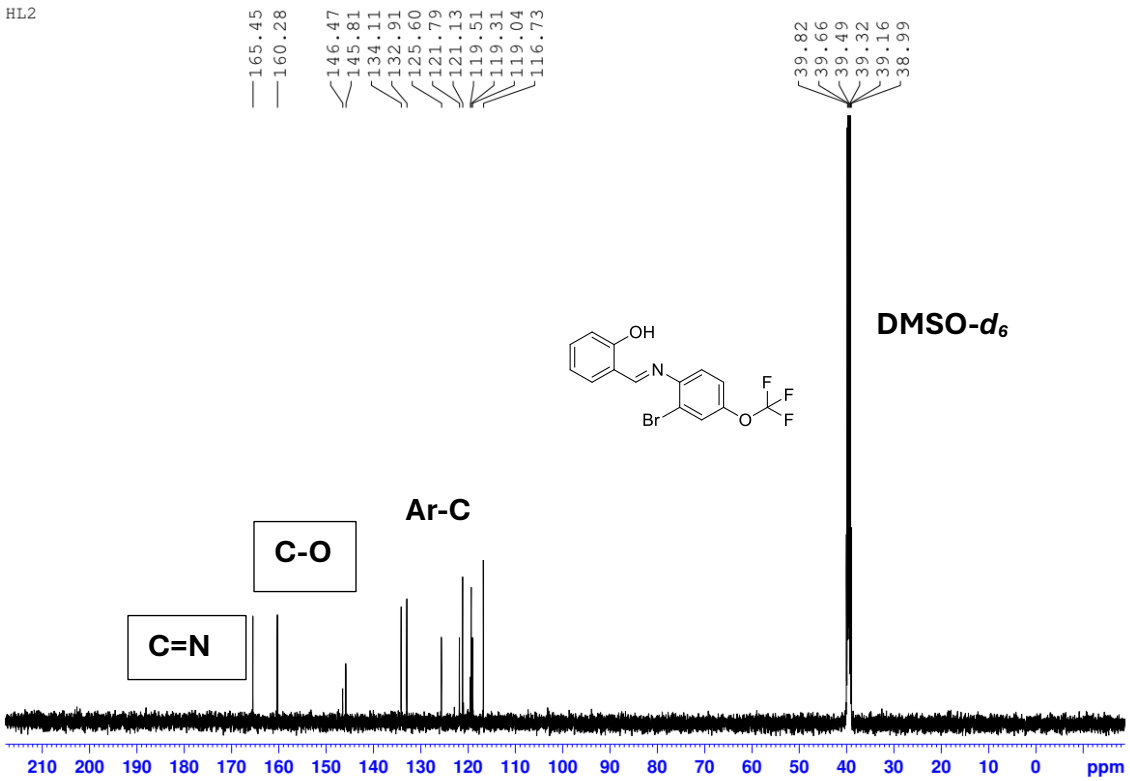

Figure S2: ^{13}C NMR spectrum of the **HL** recorded at 298 K using (125 MHz, DMSO-d_6)

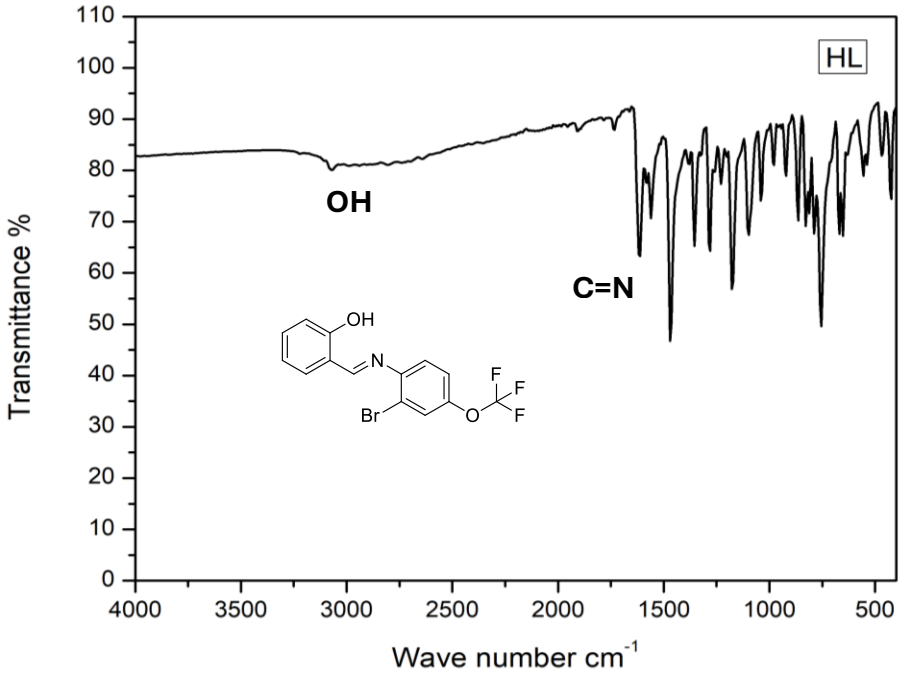

Figure S3: FTIR spectrum of **HL** recorded at solid state using ATR method at 298 K

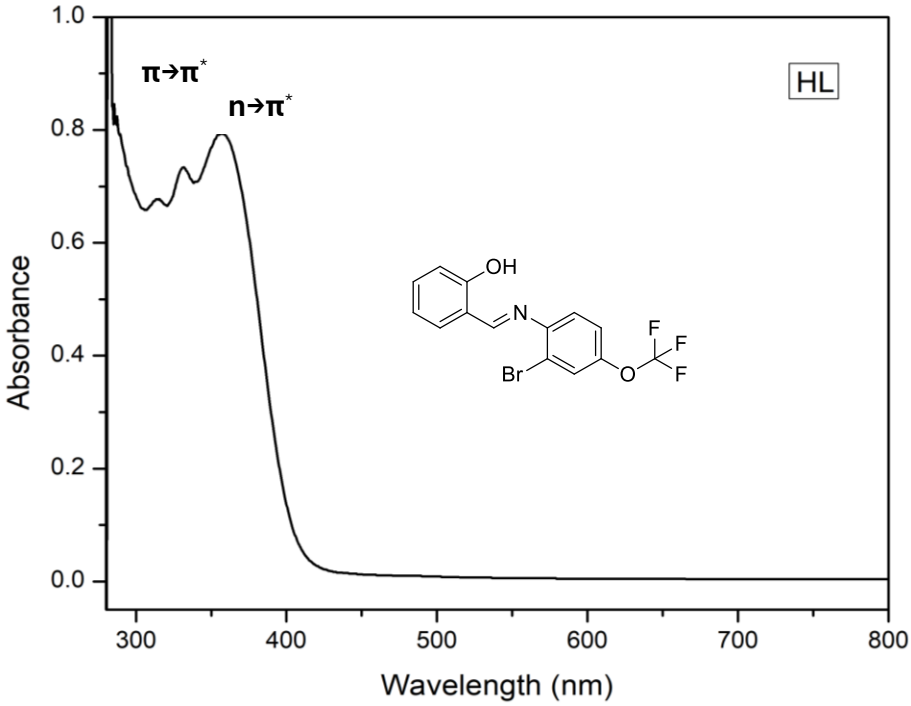

Figure S4: UV-Visible spectrum of **HL** recorded at 298 K in 10^{-3} M DMSO solution

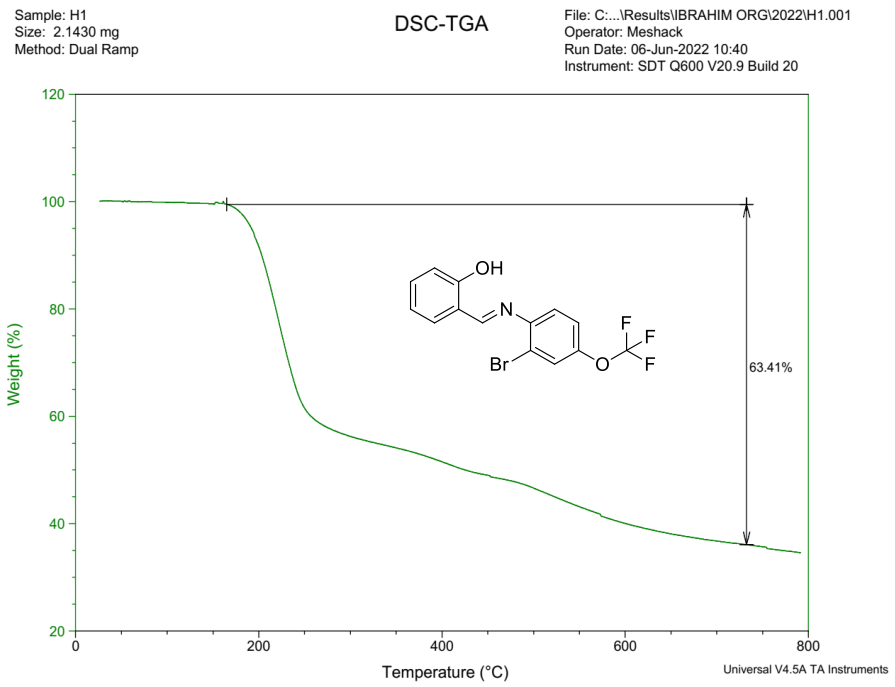

Figure S5: TGA thermogram of **HL** recorded under inert environment (N_2)

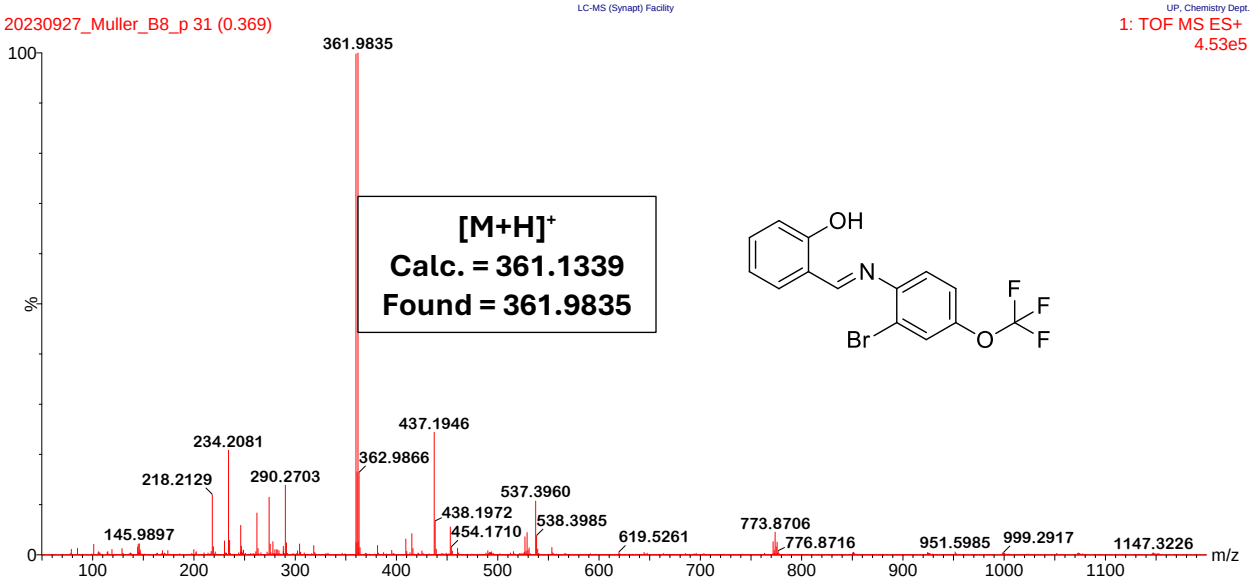

Figure S6: Mass spectrum of **HL** recorded in CH_3OH solution at 298 K using HRMS

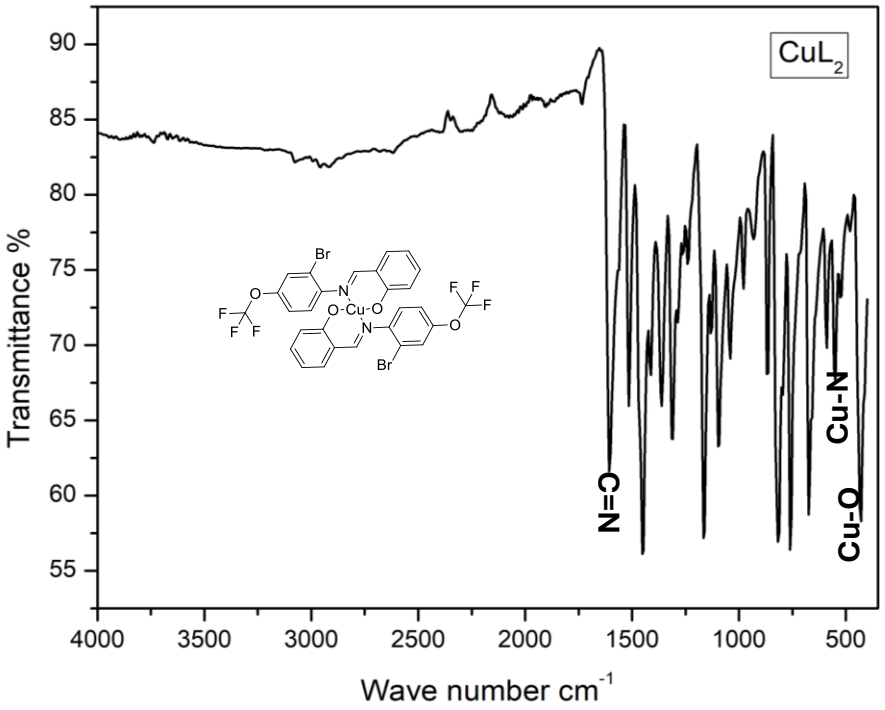

Figure S7: FTIR spectrum of **CuL_2** recorded at solid state using ATR method at 298 K

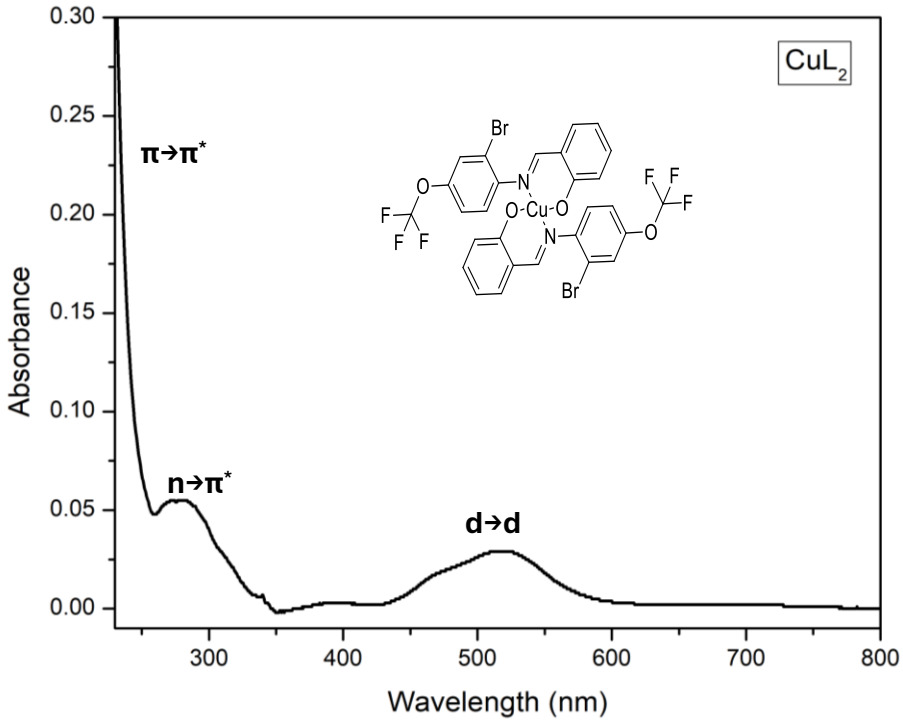

Figure S8: UV-Vis spectrum of the **CuL_2** recorded at 298 K in 10^{-3} M DMSO solution

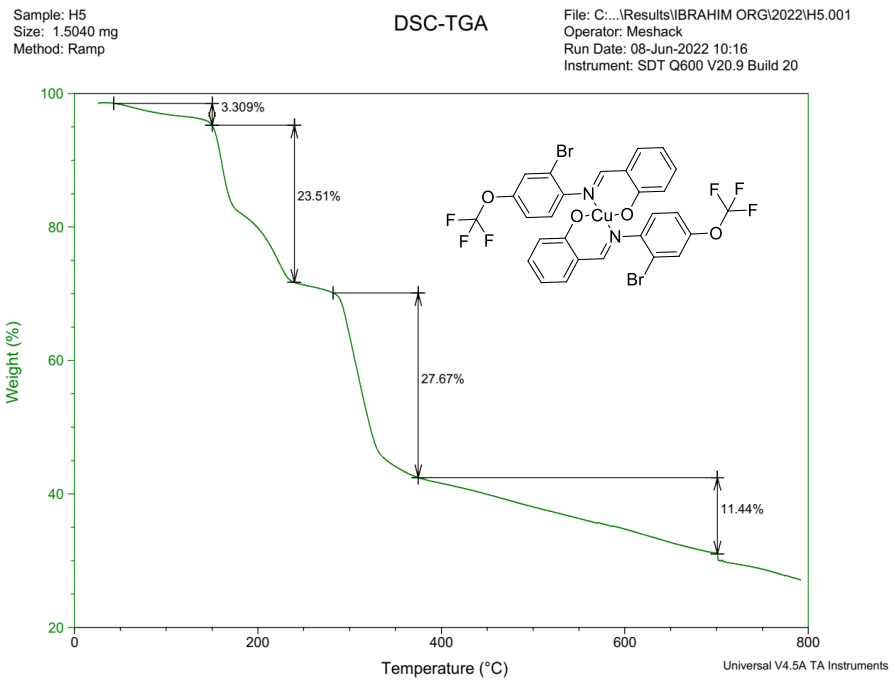

Figure S9: TGA thermograph of **CuL_2** recorded under inert environment (N_2)

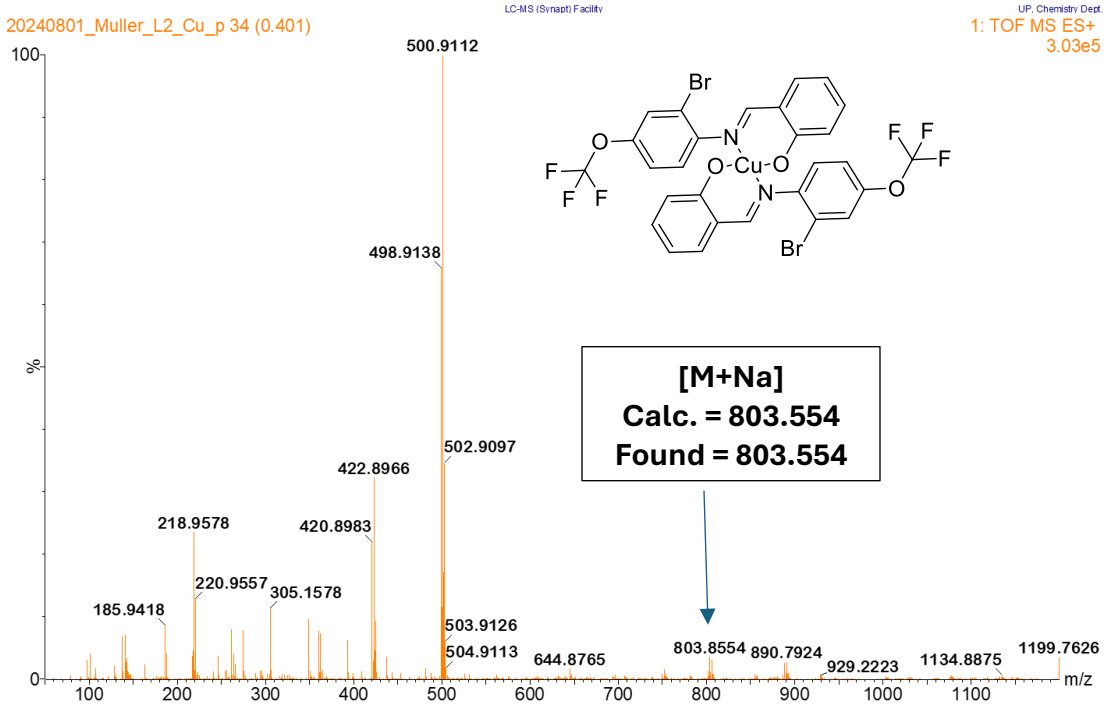

Figure S10: Mass spectrum of **CuL_2** recorded in CH_3OH solution at 298 K using HRMS

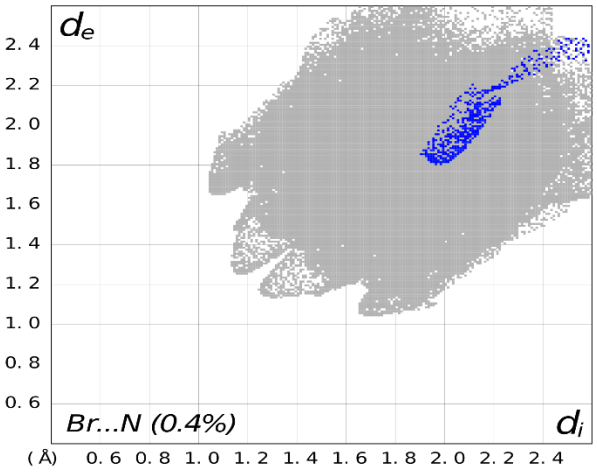
d_e
2.4
2.2
2.0
1.8
1.6
1.4
1.2
1.0
0.8
0.6
Br...N (0.4%)
d_i
(Å) 0.6 0.8 1.0 1.2 1.4 1.6 1.8 2.0 2.2 2.4

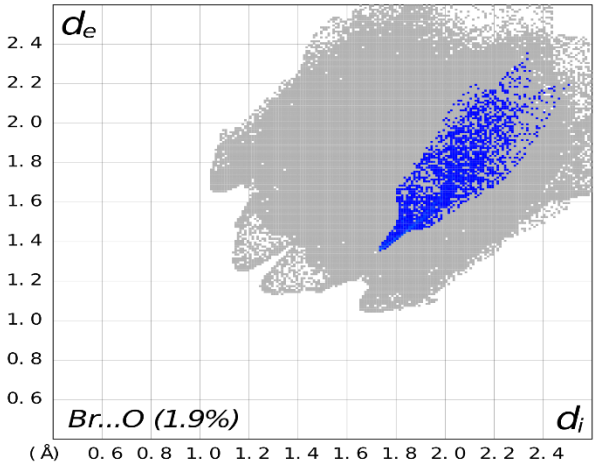
d_e
2.4
2.2
2.0
1.8
1.6
1.4
1.2
1.0
0.8
0.6
Br...O (1.9%)
d_i
(Å) 0.6 0.8 1.0 1.2 1.4 1.6 1.8 2.0 2.2 2.4

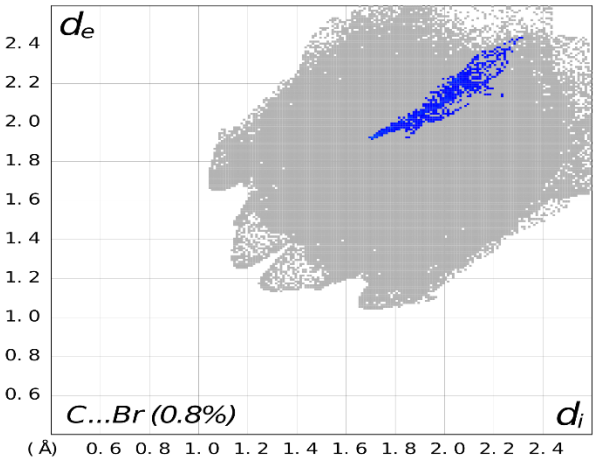
d_e
2.4
2.2
2.0
1.8
1.6
1.4
1.2
1.0
0.8
0.6
C...Br (0.8%)
d_i
(Å) 0.6 0.8 1.0 1.2 1.4 1.6 1.8 2.0 2.2 2.4

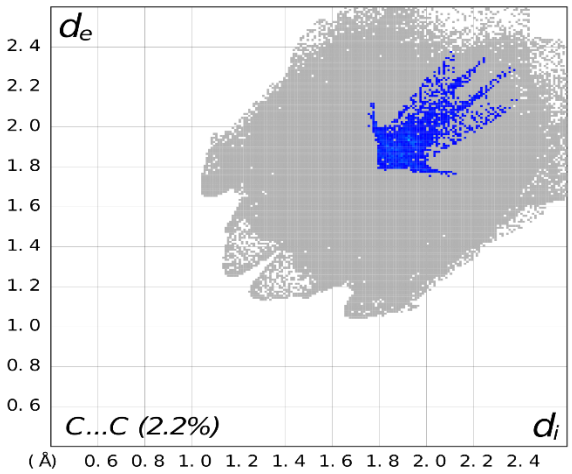
d_e
2.4
2.2
2.0
1.8
1.6
1.4
1.2
1.0
0.8
0.6
C...C (2.2%)
d_i
(Å) 0.6 0.8 1.0 1.2 1.4 1.6 1.8 2.0 2.2 2.4

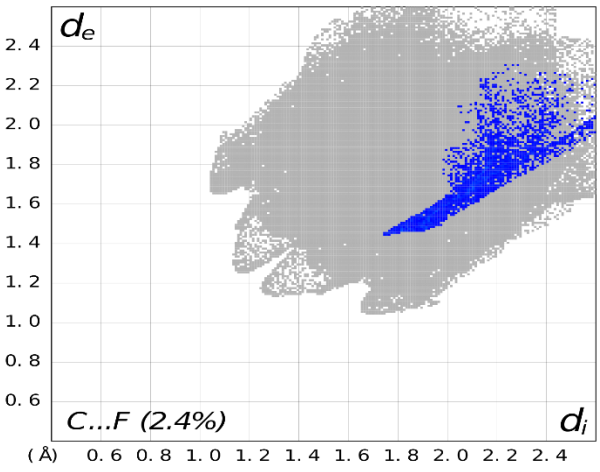
d_e
2.4
2.2
2.0
1.8
1.6
1.4
1.2
1.0
0.8
0.6
C...F (2.4%)
d_i
(Å) 0.6 0.8 1.0 1.2 1.4 1.6 1.8 2.0 2.2 2.4

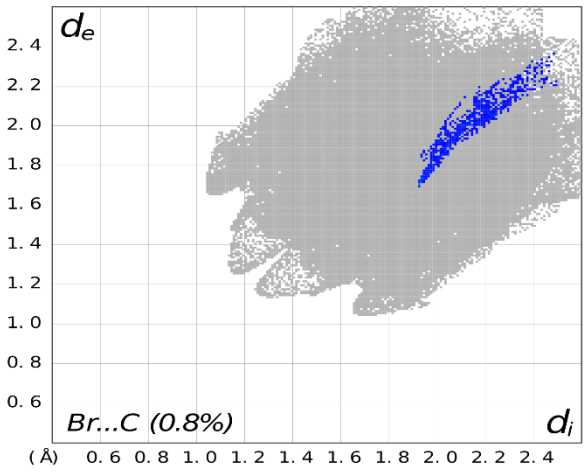
d_e
2.4
2.2
2.0
1.8
1.6
1.4
1.2
1.0
0.8
0.6
Br...C (0.8%)
d_i
(Å) 0.6 0.8 1.0 1.2 1.4 1.6 1.8 2.0 2.2 2.4

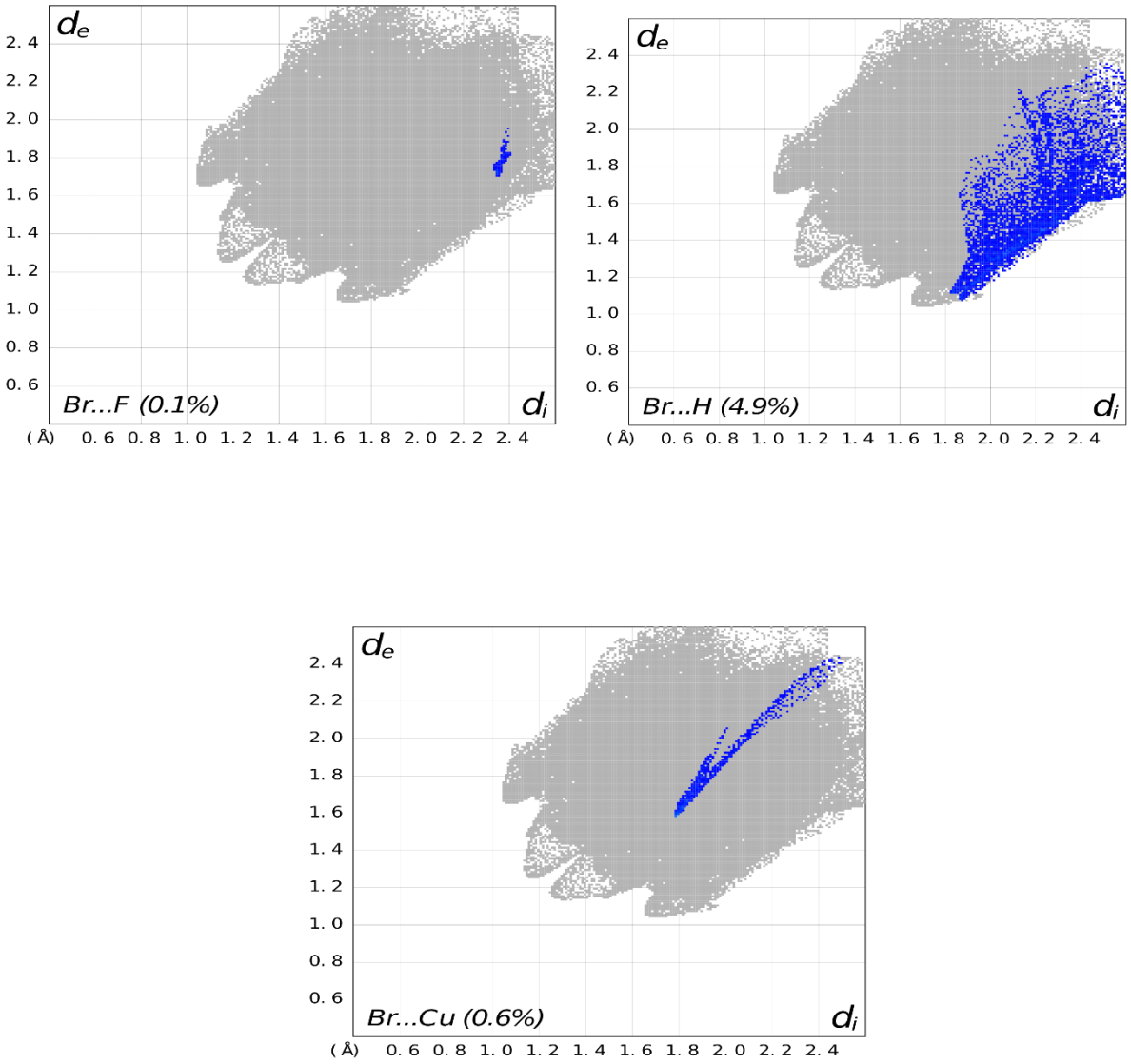

Figure S11: Two-dimensional fingerprint plots for atomic contributions during intermolecular interactions in **CuL$_2$** crystal lattice obtained at the B3LYP/6-31G(d,p) level of theory using Crystal Explorer 17.5 software.

Table S1: Crystal data and structure refinement for **CuL$_2$**

Identification code	**CuL$_2$**
Empirical formula	$C_{28}H_{16}Br_2CuF_6N_2O_4$
Formula weight	781.79
Temperature/K	173.00
Crystal system	monoclinic
Space group	$P2_1/c$

a/Å	26.7504(8)
b/Å	9.5297(3)
c/Å	11.1050(3)
α/°	90
β/°	94.9620(10)
γ/°	90
Volume/Å^3	2820.31(14)
Z	4
ρ_{calc}g/cm^3	1.841
μ/mm^{-1}	3.686
F(000)	1532.0
Crystal size/mm^3	0.236 × 0.105 × 0.069
Radiation	MoKα (λ = 0.71073)
2Θ range for data collection/°	4.54 to 55.806
Index ranges	-30 ≤ h ≤ 35, -12 ≤ k ≤ 12, -14 ≤ l ≤ 14
Reflections collected	42523
Independent reflections	6749 [R_{int} = 0.0509, R_{sigma} = 0.0323]
Data/restraints/parameters	6749/0/388
Goodness-of-fit on F^2	1.035
Final R indexes [I>=2σ (I)]	R_1 = 0.0343, wR_2 = 0.0790
Final R indexes [all data]	R_1 = 0.0445, wR_2 = 0.0836
Largest diff. peak/hole / e Å^{-3}	1.86/-0.44

Table S2. Selected Bond parameters

Bond Distances	**Length/Å**
Br(1)–C(2)	1.891(3)
Br(2)–C(16)	1.894(3)
Cu(1)–O(1)	1.8891(19)
Cu(1)–O(2)	1.8832(19)
Cu(1)–N(1)	1.988(2)
Cu(1)–N(2)	1.993(2)

Bond Distances	**Length/Å**
O(1)–C(28)	1.302(3)
Bond angles	**Angles**
O(1)–Cu(1)–N(1)	91.57(9)
O(1)–Cu(1)–N(2)	93.22(9)
O(2)–Cu(1)–O(1)	156.38(9)
O(2)–Cu(1)–N(1)	93.17(9)
O(2)–Cu(1)–N(2)	89.58(9)
N(1)–Cu(1)–N(2)	161.46(9)

Table S3: Total interaction energies for **CuL$_2$** crystal lattice at the B3LYP/6-31G(d,p) basis set

Interaction Energies (kJ/mol)
R is the distance between molecular centroids (mean atomic position) in Å.

Total energies, only reported for two benchmarked energy models, are the sum of the four energy components, scaled appropriately (see the scale factor table below)

	N	Symop	R	Electron Density	E_ele	E_pol	E_dis	E_rep	E_tot
	2	x, -y+1/2, z+1/2	10.38	B3LYP/DGDZVP	-2.3	-0.8	-14.8	11.6	-8.8
	2	x, y, z	9.53	B3LYP/DGDZVP	-17.3	-3.1	-42.7	39.3	-33.5
	2	x, -y+1/2, z+1/2	5.60	B3LYP/DGDZVP	-56.4	-7.9	-124.9	125.2	-96.9
	1	-x, -y, -z	13.89	B3LYP/DGDZVP	1.0	-0.4	-16.6	0.0	-13.8
	1	-x, -y, -z	14.09	B3LYP/DGDZVP	-3.2	-1.4	-18.5	0.0	-20.6
	2	-x, y+1/2, -z+1/2	14.58	B3LYP/DGDZVP	4.1	-0.8	-20.5	0.0	-14.1
	2	-x, y+1/2, -z+1/2	15.11	B3LYP/DGDZVP	-1.3	-0.4	-16.7	0.0	-16.2
	1	-x, -y, -z	14.41	B3LYP/DGDZVP	3.2	-0.4	-15.3	0.0	-10.3
	1	-x, -y, -z	17.01	B3LYP/DGDZVP	2.1	-0.3	-4.4	0.0	-1.9
	1	-x, -y, -z	14.60	B3LYP/DGDZVP	1.4	-0.1	-3.6	0.0	-1.7

Scale factors for benchmarked energy models
See Mackenzie et al. IUCrJ (2017)

Energy Model	k_ele	k_pol	k_disp	k_rep
CE-HF ... HF/3-21G electron densities	1.019	0.651	0.901	0.811
CE-B3LYP ... B3LYP/6-31G(d,p) electron densities	1.057	0.740	0.871	0.618

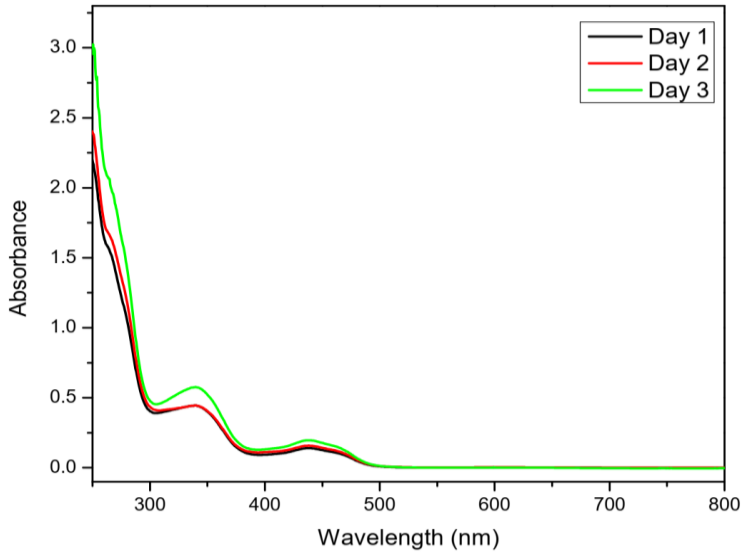

Figure S12. UV-Vis spectra of 30 μM solutions of **CuL_2** recorded as a function of time in KH_2PO_4 buffer (50 mM pH 7.5). **CuL_2** was present with a final concentration of 10% (v/v) DMSO.

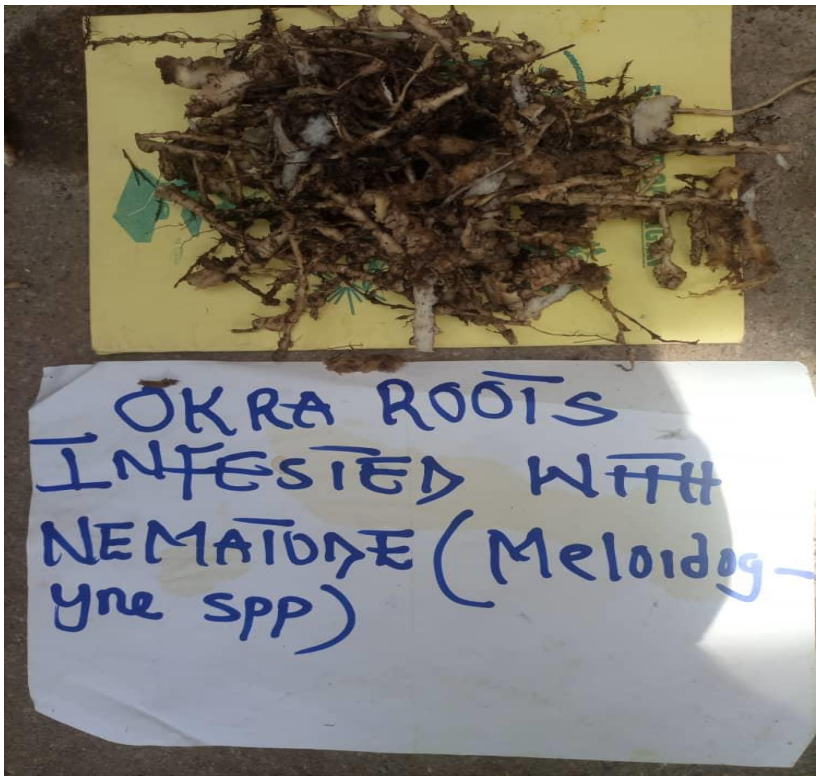

Figure S13: Nematode infected okra roots that was used to obtain the nematode eggs.

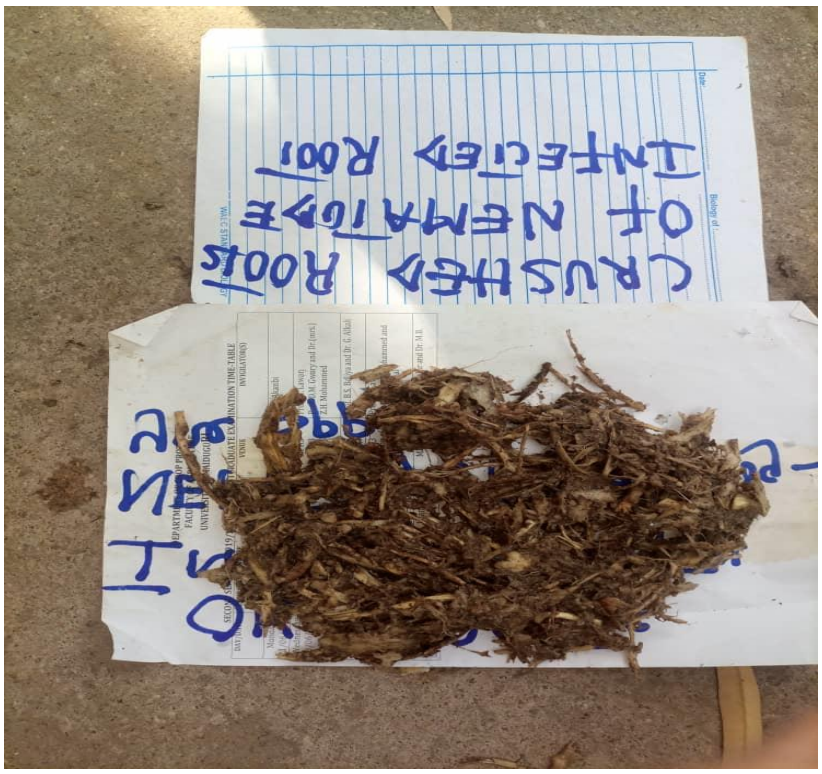

Figure S14: Crushed infected okra roots before egg extraction process.

Figure S15: The infected okra roots extracted with 200 mL of 0.5% NaOCI solution.

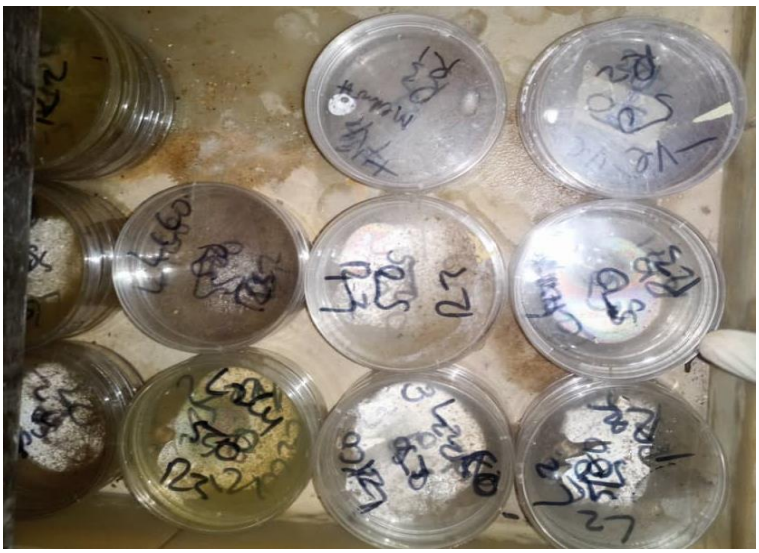

Figure S16: Extracted eggs before treatment with the compounds

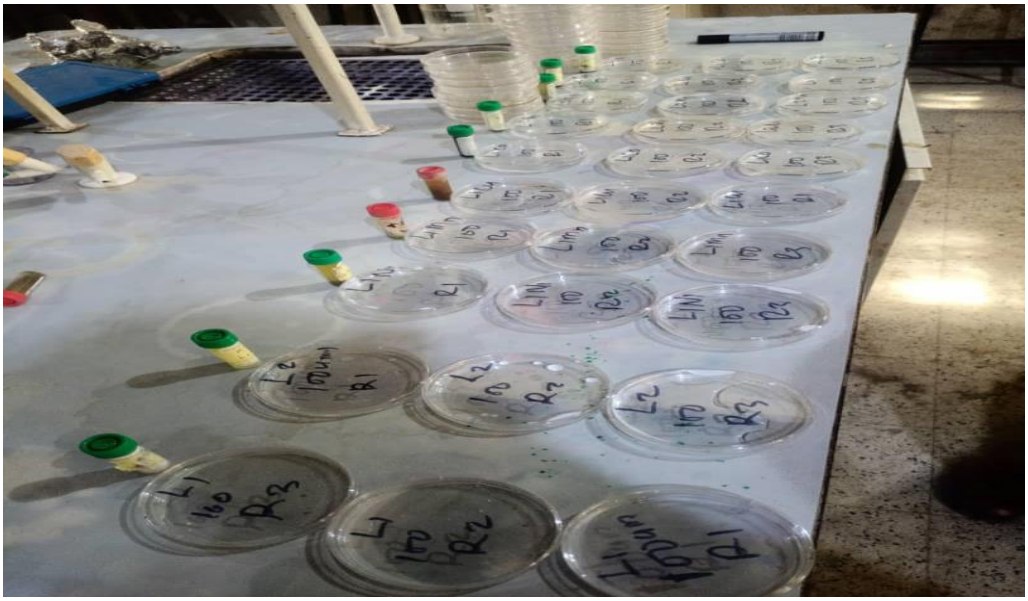

Figure S17: Extracted eggs after treatment with the compounds using concentrations of 100 µM

Figure S18: Micrograph of second stage juvenile (J2) before treatment with the compounds

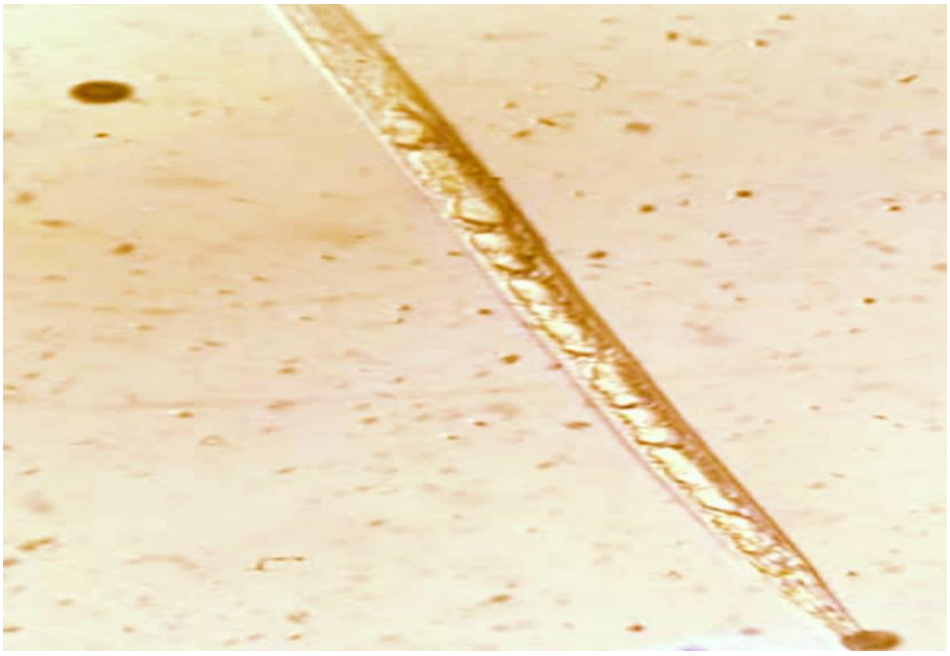

Figure S19: Micrograph of second stage juvenile (J2) after treatment with the compounds